

Synthesis, structure and spectral properties of transparent glass-ceramics based on nanocrystals of zinc aluminate spinel doped with Ti^{3+} ions

© K.N. Ereemeev¹, O.S. Dymshits^{2,3}, I.P. Alekseeva³, A.A. Khubetsov³, M.Ya. Tsenter³, S.S. Zapalova³, L.R. Basyrova³, P.A. Loiko¹, A.A. Zhilin⁴

¹ Centre de Recherche sur les Ions, les Matériaux et la Photonique (CIMAP), UMR 6252 CEA-CNRS-ENSICAEN, Université de Caen Normandie, 14050 Caen Cedex 4, France

² Ioffe Institute, 194021 St. Petersburg, Russia

³ „S.I. Vavilov State Optical Institute“, 192171 St. Petersburg, Russia

⁴ AO „D.V. Efremov Institute of Electrophysical Apparatus“, 196641 St. Petersburg, Russia

e-mail: vodym1959@gmail.com

Received December 01, 2023

Revised December 11, 2023

Accepted December 11, 2023

The structure and spectral properties of transparent glass-ceramics of the zinc aluminosilicate system containing titanium dioxide as a nucleating agent have been studied. The glass-ceramics were obtained by secondary heat-treatments of glass melted under reducing conditions and studied by differential scanning calorimetry, X-ray diffraction analysis, Raman spectroscopy, absorption and luminescence. The heat-treatments were carried out in the temperature range from 720 to 1050°C. According to the X-ray diffraction analysis, the main crystalline phase of glass-ceramics is zinc aluminate spinel (gahnite) with cubic structure and crystal size from 6 to 14 nm depending on the temperature of heat-treatment. At the temperature of 1000–1050°C crystals of TiO_2 (rutile) also appear in glass-ceramics. The volume fraction of gahnite and rutile crystals and their sizes increase with increasing temperature of heat-treatment. The lattice parameter of gahnite nanocrystals changes from 8.083 to 8.120 Å and its change occurs due to the incorporation of titanium ions. In glass-ceramics, broadband absorption in the visible and near-infrared spectral regions is observed due to the incorporation of Ti^{3+} ions into octahedral positions (positions of Al^{3+} ions) in the gahnite structure. According to Raman spectroscopy data, phase transformations in glass melted under reducing conditions are similar to those in glasses melted under oxidizing conditions, which indicates a small influence of Ti^{3+} ions on the processes of formation of glass-ceramics. Luminescence of the obtained materials is caused by superposition of luminescence of impurity Cr^{3+} ions and Ti^{3+} ions in octahedral positions in gahnite nanocrystals. The obtained regularities will be used in the development of glass-ceramics containing transition metal ions in lower oxidation states.

Keywords: transparent glass-ceramics, nanocrystals, zinc aluminate spinel, titanium ions, structure, optical spectroscopy, X-ray diffraction analysis, Raman spectroscopy.

DOI: 10.61011/EOS.2024.02.58450.5815-23

Introduction

An important task is the development of phosphors that do not contain ions of rare earth elements [1]. Ions Ti^{3+} in crystals and glasses demonstrate broadband luminescence in the visible and near IR ranges of the spectrum [1,2] and are of interest for development of tunable lasers. After development of solid-state lasers of wide spectral range based on sapphire crystals $\alpha-Al_2O_3$ doped with Ti^{3+} [3–6] ions, the optical properties of Ti^{3+} ions in different optical materials became the focus of attention [7–10]. In particular, the magnesium aluminate spinel single crystals, $MgAl_2O_4$, doped with Ti^{3+} ions were obtained and studied [11,12]. Zinc aluminate spinel,

$ZnAl_2O_4$, gahnite, is also an aluminate spinel. It demonstrates promising optical, catalytic, dielectric properties, radiation resistance and high doping capacity for transition metal ions [13–18]. Since the growth of gahnite single crystals is a technologically complicated task, it seems promising to develop transparent glass-ceramics based on gahnite [19,20]. Until now it was assumed that it was not possible to synthesize the gahnite crystals doped with Ti^{3+} ions [17,18].

The goal of this study is to develop and study the transparent glass-ceramics containing Ti^{3+} ions in gahnite nanocrystals. This study is important for development of phosphors free of rare-earth ions.

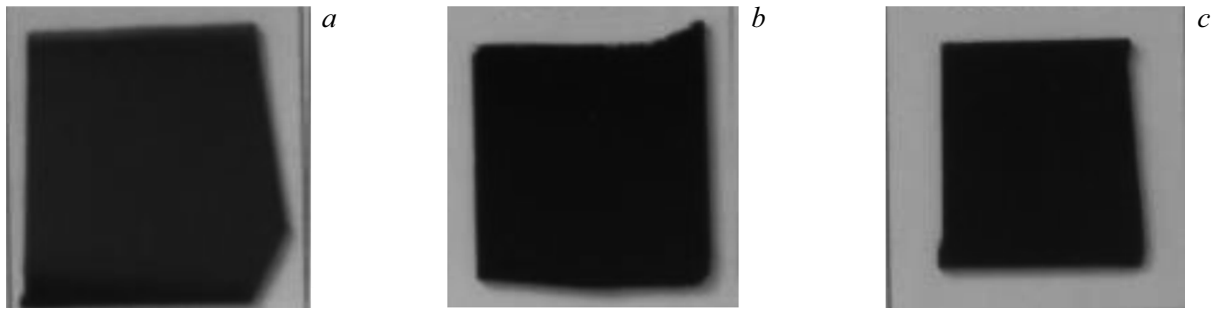


Figure 1. Photos of the polished initial glass (a) and glass-ceramics (b, c), produced by two-stage heat-treatment with the first hold at 720°C, second one at 750°C (b) and 1000°C (c). The heat-treatment time at each stage is 6 h. Sample thickness is 1.0 mm.

Materials and methods

The paper investigated the model ceramizing glass of zinc-alumosilicate system with addition of titanium dioxide as a nucleating agent and glass-ceramics produced as a result of its secondary heat-treatments. Titanium dioxide served not only as a nucleating agent, but as a source of Ti^{3+} ions as well. The glass with composition of 25 ZnO, 25 Al_2O_3 , 50 SiO_2 , 9 TiO_2 (mol%) [19–22] and 400 g in weight was melted in reducing conditions (with addition of coal in the batch) in a crucible made of quartz ceramics in the laboratory glass melting furnace at 1580°C with stirring for 4 h. The glass melt was poured onto a massive metal plate, and the glass was annealed at 660°C for 1 h with subsequent cooling with the annealing furnace.

The glass was cut with a diamond saw into samples that were heat-treated in two-stage schedules in the Nabertherm heat-treatment furnace. Based on the previous studies [1–4], the first stage of heat-treatment, so called nucleation, was carried out at 720°C for 6 h. High-temperature heat-treatment at the crystallization stage was carried out at temperature from 750 to 1050°C for 6 h.

As a result, transparent materials of grey and black color were obtained, the color intensity of which increased as the heat-treatment temperature was rising (Fig. 1).

The sequence of phase transformations occurring upon heating of the initial glass and the glass subjected to the nucleation heat-treatment at 720°C for 6 h, was studied by the method of differential scanning calorimetry (DSC) using a differential scanning calorimeter Netzsch STA 449 F3 Jupiter with dynamic flow of Ar. The DSC curves were recorded in the temperature range of 20–1200°C with the rate of 10°C per second. The glass transition temperature, T_g , the onset crystallization temperature, T_{on} , and temperature of crystallization maximum, T_m , were determined in Proteus software with error $\pm 1^\circ C$.

Powder X-ray diffraction (XRD) patterns of the glass and glass-ceramics were recorded using a diffractometer Shimadzu 6000, irradiation $CuK\alpha$ ($\lambda = 1.5406 \text{ \AA}$) with Ni filter in the angular range of $2\theta = 10\text{--}80^\circ$ with pitch 0.02° and rate of 2° per minute. The average diameter of the gahnite crystals was determined from the line with Miller's

indices (440) $2\theta = 65.5^\circ$ using the Scherrer's equation [23]:

$$D_{XRD} = \frac{K\lambda}{\beta(2\theta) \cos \theta}, \quad (1)$$

where D_{XRD} — average diameter of crystals (in \AA); K — dimensionless coefficient of particle shape ($K \approx 1$); λ — X-ray wavelength; β — peak width at half of its maximum in radians; θ — angle of diffraction, ° (Bragg angle).

The error of determination of the average diameter of nanocrystals depends on their size. In this case the diameter of nanocrystals was determined with the accuracy of 10%.

The lattice parameter a of $ZnAl_2O_4$ was determined from the line with the Miller indices (440) $2\theta = 65.5^\circ$ using the formula:

$$a = d_{(440)}\sqrt{32}, \quad (2)$$

where a — lattice parameter of $ZnAl_2O_4$, \AA ; $d_{(440)}$ — interplanar spacing. The error of detecting the parameter a is $\pm 0.003 \text{ \AA}$.

Raman spectra of the initial and heat-treated glasses were measured for the specially made flat parallel polished samples with size of $25 \times 15 \text{ mm}$ and thickness of 1 mm at room temperature using a micro-Raman spectrometer InVia Renishaw in the geometry of back scattering of light using an edge filter. The Raman spectra were recorded with 30 accumulations of the signal. Raman spectra were excited by radiation of an Ar^+ gas laser at wavelength 514 nm. Photoluminescence spectra were also measured using this spectrometer with the excitation wavelength 457 nm of the same laser.

The absorption spectra of the initial and heat-treated glasses were recorded in a spectrophotometer Shimadzu UV 3600 in the spectral range of 250–2500 nm with a step of 1 nm. The samples used were flat parallel polished plates with size of $25 \times 15 \text{ mm}$ and thickness of 1 mm. The natural coefficient of absorption at the wavelength λ was determined using the formula

$$\alpha_\lambda = 23 \frac{(D_\lambda - \Delta)}{l}, \quad (3)$$

D_λ — optical density of the sample at wavelength λ ; Δ — losses of light in the sample (reflection from parallel

surfaces, scattering on glass defects and crystals, light absorption by unwanted impurities); l — sample thickness, mm.

The value Δ was determined experimentally as light losses in the initial glass in the spectral range, where there is no light absorption by the color centers (the wavelength was chosen as 2200 nm), and was used to calculate the absorption coefficients of initial and heat-treated glasses.

Results

Fig. 2 presents the DSC curves of the initial glass and glass after nucleation heat-treatment at 720°C for 6 h. These curves differ from each other significantly. There is a single intense and narrow exothermic peak observed in the DCS curve of the initial glass. According to the data of the papers [3,4], this peak is due to the gahnite crystallization. The glass transition temperature of the initial glass is $T_g = 695^\circ\text{C}$, the onset crystallization temperature is $T_{on} = 812^\circ\text{C}$, and the temperature of crystallization maximum is $T_{max} = 839^\circ\text{C}$. DCS curve of the sample heat-treated at 720°C for 6 h, is noticeably different from the DSC curve of the initial glass. After the preliminary heat-treatment, the exothermic peak caused by gahnite crystallization becomes wider and more intense. It occurs at the temperature that is approximately 40°C lower than the peak on the DSC curve of the initial glass, in this case $T_{on} = 755^\circ\text{C}$, and $T_{max} = 795^\circ\text{C}$. Therefore, nucleation heat-treatment significantly affects the glass structure. It is worth mentioning that the glass transition temperature T_g increases slightly after this heat-treatment and equals to 698°C.

Fig. 3 presents XRD patterns of the initial and heat-treated glasses. The initial glass is X-ray amorphous, the maximum of amorphous halo is observed at the angle of diffraction $2\theta = 25.4^\circ$. Nucleation at 720°C for 6 h results in appearance of traces of gahnite nanocrystals with the cubic spinel structure. After the heat-treatment at 750°C

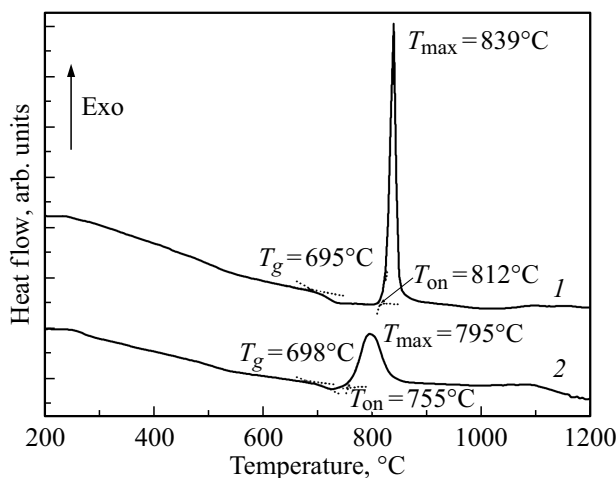


Figure 2. Curves of differential scanning calorimetry: 1 — sample of initial glass, 2 — sample heat-treated at the nucleation stage at 720°C for 6 h.

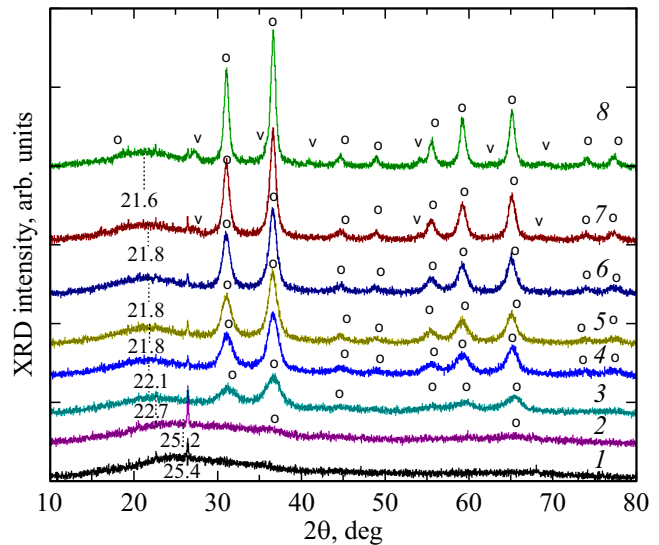


Figure 3. XRD patterns of the samples of initial (1) and heat-treated (2–8) glasses. Heat-treatment schedules: 2 — 720°C, 3 — 720 + 750°C; 4 — 720 + 850°C; 5 — 720 + 900°C; 6 — 720 + 950°C; 7 — 720 + 1000°C; 8 — 720 + 1050°C. Heat-treatment time at each stage is 6 h. Legend: o — peaks related to crystals $\text{Ti}_3\text{ZnAl}_2\text{O}_4$; v — peaks related to crystals TiO_2 (rutile).

at the second stage, the composition of the residual glass remains close to that for quartz glass, since the maximum of amorphous halo moves to $2\theta = 22.7^\circ$ (Fig. 3). The samples produced by two-stage heat-treatment with the second stage temperature up to 950°C inclusive contain the only crystalline phase — gahnite. The volume fraction of gahnite crystals increases with the increase of the heat-treatment temperature at the second stage (Fig. 4, a), and the average crystal size rises from 6 to 14 nm (Fig. 4, b). The gahnite lattice parameter a varies from 8.084 Å in the material produced by heat-treatment at the second stage at 750°C, to the maximum value of 8.119 Å (heat-treatment at 900°C) and reduces to the value of 8.109 Å as a result of heat-treatment at 1050°C (Fig. 4, c). As a result of heat-treatment at 1000 and 1050°C the XRD patterns additionally show weak diffraction peaks of stable modification of TiO_2 , rutile (Fig. 3).

Raman spectroscopy is an effective method to study liquid phase separation occurring upon appearance and development of titanium-containing amorphous phase in titania-doped glasses [2]. Raman spectra of the initial glass and glass-ceramics are shown in Fig. 5.

The Raman spectrum of the initial glass contains wide bands, low frequency one at $\sim 455\text{ cm}^{-1}$ and two high frequency ones at ~ 800 and $\sim 920\text{ cm}^{-1}$. Bands ~ 455 and $\sim 800\text{ cm}^{-1}$ refer to the vibrations of aluminosilicate lattice tetrahedrons in the glass structure, and the band $\sim 920\text{ cm}^{-1}$ is related to the vibrations of tetrahedrons $[\text{TiO}_4]$, built into this lattice [2].

After the heat-treatment of the initial glass at 720°C for 6 h a small shift of the band is observed from ~ 455

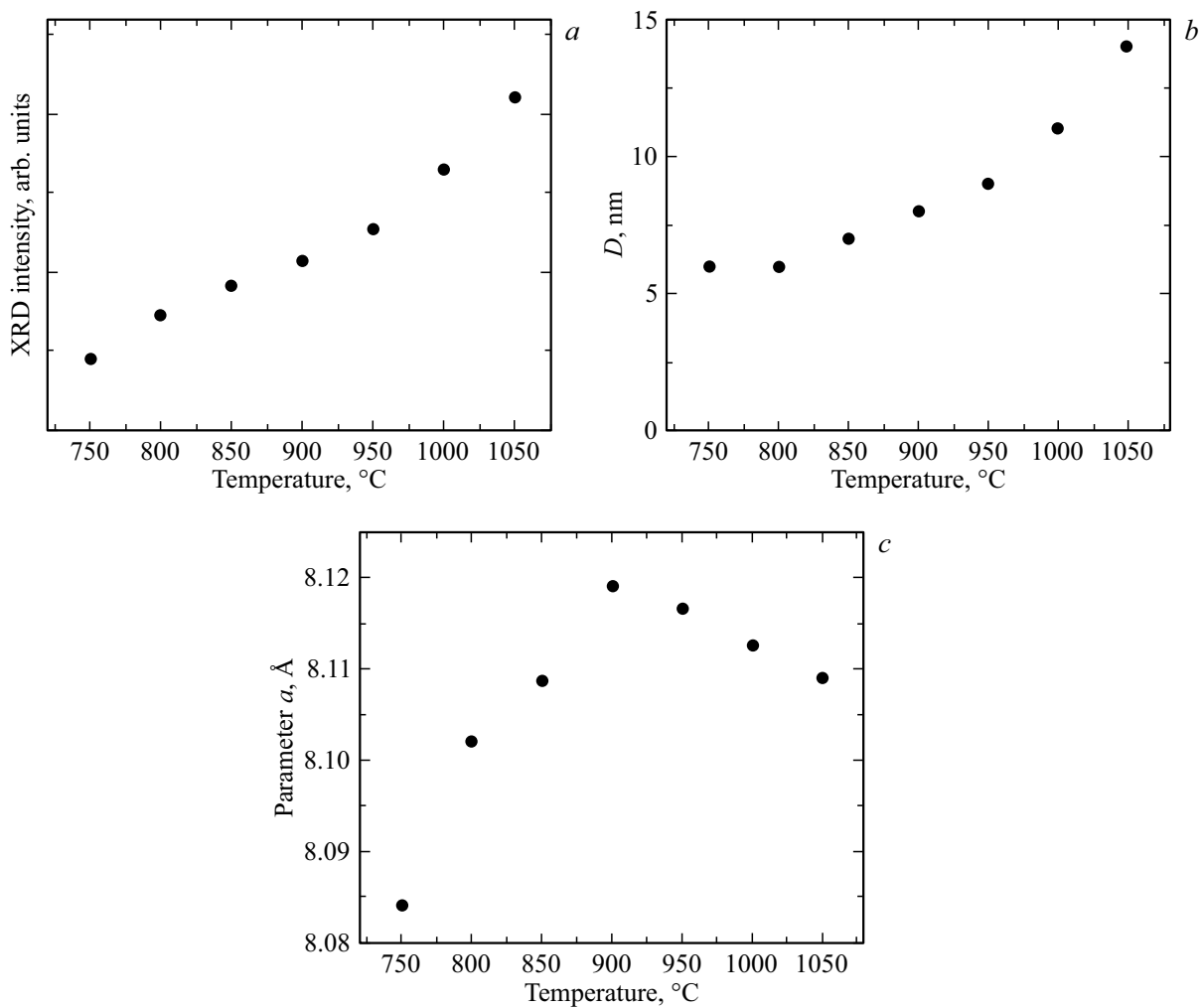


Figure 4. The analysis of the XRD data (*a*) intensity of diffraction peak of gahnite with Miller index (*hkl*) (311); *b* — average size of gahnite crystals; *c* — gahnite lattice parameter *a* depending on the heat-treatment temperature at the second stage. Heat-treatment at the nucleation stage is 720°C. Heat-treatment time at each stage is 6 h.

to $\sim 446\text{ cm}^{-1}$, and the distribution of the intensities changes in the high frequency bands: the band with the maximum at 800 cm^{-1} increases compared to the band with maximum at 920 cm^{-1} , which means the beginning of liquid phase separation of the initial glass [20].

After the two-stage heat-treatment with temperature 750°C at the second stage one may observe in the Raman spectrum the shift of the band maximum position at ~ 800 to $\sim 790\text{ cm}^{-1}$ and the growth of band intensities with maxima at ~ 446 and $\sim 790\text{ cm}^{-1}$. Besides, the band in the range of $\sim 930\text{ cm}^{-1}$ nearly disappears. These changes are related to the development of the liquid phase separation and continuation of the formation of zincaluminotitanate liquid phase separated regions [20]. The intense band with the maximum at $\sim 790\text{ cm}^{-1}$, related to the vibrations of groups $[\text{TiO}_5]$ and $[\text{TiO}_6]$ in these regions, is imposed upon the weak band at 800 cm^{-1} , related with the vibrations of aluminosilicate lattice tetrahedrons in the initial glass. Weak bands also appear at 196, 419 and 658 cm^{-1} ,

due to the vibrations in gahnite nanocrystals [22]. In Raman spectra of samples prepared by heat-treatment at the second stage at the temperature 850–1050°C, the bands are increased in intensity, which belong to the vibrations in the gahnite crystals [22], and bands also appear at ~ 714 and $\sim 786\text{ cm}^{-1}$, provided for by appearance of a partially inverse structure of these crystals [24,25]. Weak bands at ~ 940 and $\sim 1106\text{ cm}^{-1}$ in the high-frequency range of Raman spectrum are related to the vibration modes of the isolated titanium centers Ti^{4+} in the residual glass [20]. After the heat-treatment at the second stage at temperatures 1000 and 1050°C the gahnite band intensity in the spectra increases, and the intensity of the wide band 786 cm^{-1} gradually decreases. Vibrations appear and strengthen at 144, ~ 238 , 440 and 608 cm^{-1} , due to the rutile crystallization [20]. The obtained data are not only compliant with the XRD analysis data, but also make it possible to follow the transformations in the liquid phase separated titanate phase.

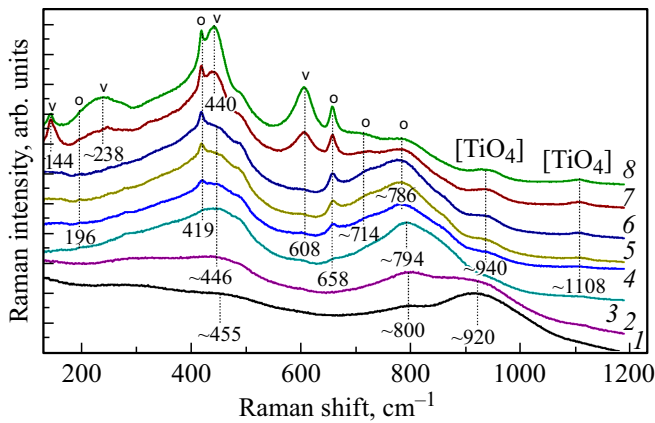


Figure 5. Raman spectra of the samples of initial (1) and the heat-treated (2–8) glasses. Heat-treatment schedules: 2 — 720°C, 3 — 720 + 750°C; 4 — 720 + 850°C; 5 — 720 + 900°C; 6 — 720 + 950°C; 7 — 720 + 1000°C; 8 — 720 + 1050°C. Heat-treatment time at each stage is 6 h. The excitation wavelength is 514 nm. Legend: o — vibrations related to crystals $\text{Ti:ZnAl}_2\text{O}_4$; v — vibrations related to crystals TiO_2 (rutile).

The absorption spectra of the initial glass, the glass after the nucleation heat-treatment and glass-ceramics produced by two-stage heat-treatment in the temperature range at the second stage 750–1050°C, are provided in Fig. 6, a, b.

It is known that the titanium ions in glasses exist in two oxidation states, Ti^{3+} (electron configuration $3d^1$) and Ti^{4+} (electron configuration $3d^0$). The ion Ti^{3+} in the ligand field may have two absorption bands. The wide asymmetric band caused by transition ${}^2T_{2g} \rightarrow E_g$ of ions Ti^{3+} in octahedral (O_h) symmetry in silicate glasses is usually located in the spectral area from 480 to 700 nm depending on the ligand field strength and extent of distortion of its symmetry [8]. Absorption with the maximum at the wavelength ~ 800 nm is caused by pairs $\text{Ti}^{3+}-\text{Ti}^{4+}$ [26]. The band caused by the transition $E_g \rightarrow 2T_{2g}$ of ions Ti^{3+} in the ligand field of tetrahedral (T_d) symmetry is located at about 1000 nm [27]. The oxygen — metal charge transfer band from the oxygen ions to the titanium ions Ti^{3+} (OMCT) $\text{O}-\text{Ti}^{3+}$ is in the UV spectral range at ~ 240 nm [28]. Because of unfilled $3d$ -orbitals the ions Ti^{4+} have no $d-d$ -transitions. The oxygen — metal charge transfer band from the oxygen ions to the titanium ions Ti^{4+} (OMCT) $\text{O}-\text{Ti}^{4+}$ is in the UV spectral range at the wavelength of around 300 nm [29].

In different minerals the intervalence charge transfer $\text{Ti}^{4+}-\text{Ti}^{3+}$ (IVCT) results in appearance of the absorption band in the range ~ 480 nm [29] or 660–670 nm [30].

In the spectrum of the initial glass the absorption edge defined as the value of the wavelength produced when crossing the straight line tangent to UV edge of the absorption spectrum, with axis x , is at the wavelength 340 nm (Fig. 6, b). In this spectrum we also observe the nonstructured absorption band in the range from ~ 370 to 1200 nm with maximum at ~ 494 nm, related to absorption of ions Ti^{3+} in the distorted octahedral (transition

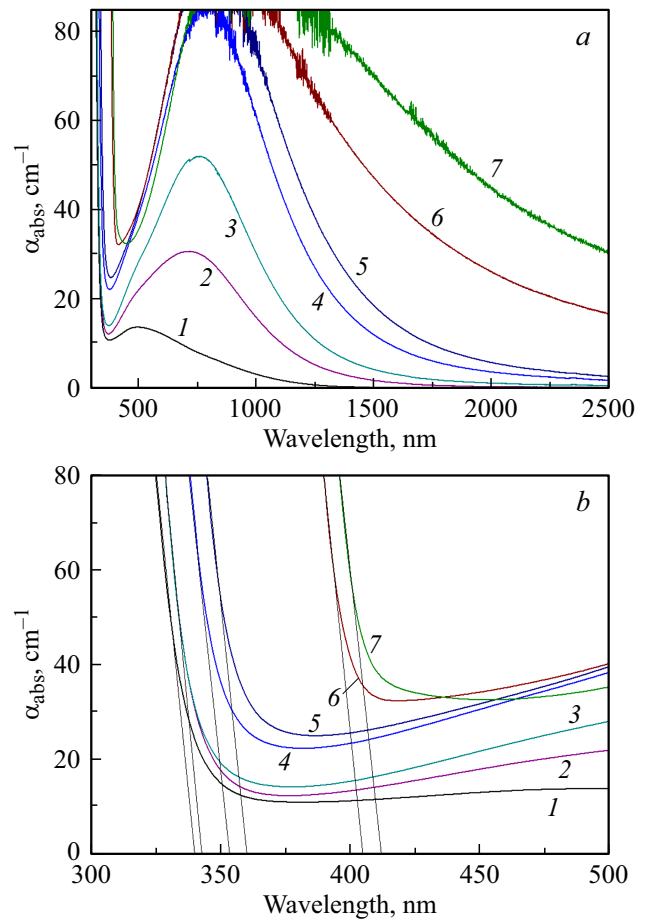


Figure 6. Absorption spectra of the samples of initial (1) and heat-treated (2–7) glasses (a) in the wavelength range 300–2500 nm; b — in the wavelength range 300–500 nm. Heat-treatment schedules: 2 — 720°C, 3 — 720 + 750°C; 4 — 720 + 850°C; 5 — 720 + 950°C; 6 — 720 + 1000°C; 7 — 720 + 1050°C. Heat-treatment time at each stage is 6 h.

$T_{2g} \rightarrow E_g$) and, possibly, to some extent, in the tetrahedral coordination (transition $E_g \rightarrow 2T_{2g}$) in the initial zincaluminosilicate glass. After nucleation of the initial glass, its absorption spectrum shows a slight shift of the absorption edge from 340 to 343 nm, increased intensity and widening of the absorption band located in the visible and near IR spectral range (up to 1500 nm). The maximum of this wide absorption band is at 725 nm.

The absorption edge in the spectrum of the sample produced by the two-stage heat-treatment with temperature 750°C at the second stage matches the position of the absorption edge in the spectrum of the glass heat-treated at the nucleation stage, and is at 343 nm. The absorption edge in the spectrum of the sample produced by two-stage heat-treatment with temperature 850°C at the second stage is observed at 353 nm. Rise in the temperature of heat-treatment at the second stage up to 900, 950, 1000 and 1050°C results in the shift of the absorption edge to the values of 353, 350, 405 and 412 nm accordingly (Fig. 6, b).

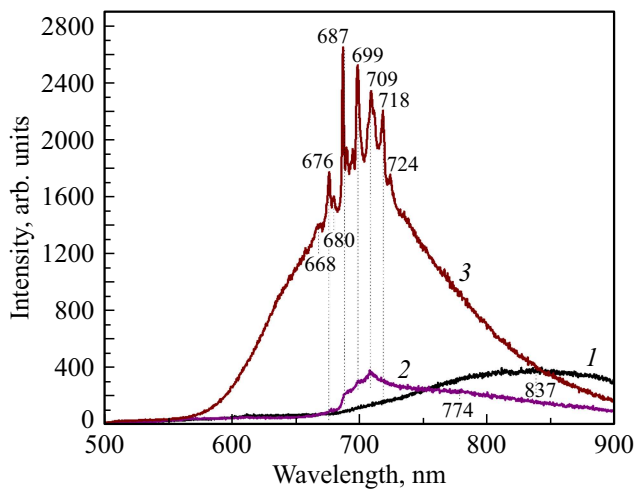


Figure 7. Luminescence spectra of the initial glass (1), of the sample produced by heat-treatment at 720 (2), at 720 and 1000°C (3). The excitation wavelength is 457 nm. Heat-treatment time at each stage is 6 h.

In the spectra of glass-ceramics the unstructured and wideband absorption in the visible and near IR regions becomes more intense with the raise of heat-treatment temperature at the second stage, and the absorption maximum position moves to longer wavelengths, namely from ~ 760 nm (heat-treatment at 750°C) to ~ 917 nm (heat-treatment at 1050°C). Such band may be related to absorption caused by ions Ti^{3+} in octahedral coordination (transition $T_{2g} \rightarrow E_g$), and intervalence charge transfer (IVCT) $\text{Ti}^{3+}-\text{Ti}^{4+}$ [7].

Luminescence spectra of the initial glass, the glass subjected to the heat-treatment at the nucleation stage and the glass-ceramic produced by heat-treatment of the initial glass at 1000°C, are shown in Fig. 7. The luminescence spectrum of the initial glass is a wide non-structured band with maximum at ~ 837 nm. After heat-treatment at 720°C the substantial changes occur in the luminescence spectrum — the maximum disappears at 837 nm, a weak non-structured band occurs at about 700 nm with maxima at 680, 687, 699, 709 and 718 nm, and also a tail stretching to 900 nm, and with maximum at 774 nm. The spectrum of the sample obtained by heat-treatment at 1000°C, represents a wide intense band in the range from 570 to 900 nm with maxima at 668, 680, 687, 699, 709, 718 and 724 nm.

Discussion

The sequence of phase transformations observed during the heat-treatment of the initial glass produced in reducing conditions is similar to such for ceramizing titanium-containing glasses of zincaluminosilicate system melted under oxidizing conditions [19,20]. In particular, the Raman spectrum of the initial glass indicates the presence of complexes $[\text{Ti}^{4+}\text{O}_4]^{4-}$ in it. Therefore, it may be assumed

that the fraction of ions Ti^{4+} in the glass obtained under reducing conditions is prevalent, and it determines the process of liquid phase separation that results in gahnite crystallization when the temperature of the secondary heat-treatment rises. Nevertheless, the absorption spectrum of the initial glass indicates the presence of ions Ti^{3+} in the glass in the octahedral ligand field (Fig. 6). Appearance of gahnite nanocrystals, the traces of which are even found in the sample heat-treated at 720°C, and the raise of their volume fraction when heat-treatment temperature increase result in the growth of the absorption intensity caused by the ions Ti^{3+} , entering into these crystals.

According to the literature data, the lattice parameter of gahnite is 8.086 Å (PDF#74-1136). Gahnite that crystallizes at the heat-treatment temperature of 750°C, corresponds to normal spinel with low degree of inversion [31]. Increase of the heat-treatment temperature to 900°C causes considerable increase of the lattice parameter a to the value of 8.120 Å. Upon further increase of heat-treatment temperature the value of the parameter a somewhat reduces, being much higher than the value characteristic for normal spinel. The growth of the spinel lattice parameter may be related to the content of titanium ions in its structure with different valences, not only Ti^{4+} , but also Ti^{3+} .

Narrow lines in the luminescence spectrum of glass-ceramic produced by heat-treatment at 1000°C, comply with the luminescence spectrum of chromium ions Cr^{3+} in octahedral O_h sites in gahnite nanocrystals [32,33]. It means that the change in the luminescent properties of the initial glass during heat-treatment should be related to extrinsic ions Cr^{3+} , which are located in different phases of multiphase materials. Note that chromium ions are an unwanted impurity in zinc and aluminium oxides [33]. The luminescence spectrum of the initial glass is similar to the luminescence spectra of silicate glasses containing Cr^{3+} ions in the distorted octahedral symmetry in the weak ligand field [34]. Appearance of spectral signs of Cr^{3+} ions in the crystals of zinc aluminate spinel after heat-treatment at 720°C is confirmed by the data of XRD analysis on crystallization of small quantities of gahnite during this heat-treatment. In the luminescence spectrum of the glass-ceramic prepared by heat-treatment at 1000°C, narrow peaks at wavelengths 668, 680, 687, 689, 695, 698, 709, 718 and 724 nm are on the background of a wide non-structured luminescence band with the maximum in the range of 700 nm, caused evidently by Ti^{3+} ions in gahnite [2] nanocrystals and Cr^{3+} ions in the residual glass.

Conclusions

Phase transformations were studied in titanium-containing glasses of the zincaluminosilicate system melted under reducing conditions. It was found that the reducing melting conditions impact the character of phase transformations.

Raman spectra demonstrated that the initial glass had complexes $[\text{Ti}^{4+}\text{O}_4]^{4-}$, and their fraction was high. A larg

fraction of Ti^{4+} ions in the initial glass plays a decisive role in the phase decomposition kinetics.

The absorption spectrum of the initial glass indicates the presence of Ti^{3+} ions in the glass in the octahedral ligand field. In the absorption spectra of samples prepared by secondary heat-treatment, the increase of intensity of absorption caused by ions Ti^{3+} is observed.

As the heat-treatment temperature increases, gahnite nanocrystals appear and grow in the glass. Titanium ions enter into the composition of gahnite crystals, which is confirmed by the increase in the lattice parameter. As the volume fraction of gahnite crystals grows with rising temperature, the fraction of Ti^{3+} ions in the gahnite structure increases too.

Luminescent properties of the studied material when excited by a laser with excitation wavelength 453 nm are determined by extrinsic ions Cr^{3+} and Ti^{3+} in octahedral positions in the gahnite crystals.

This study was supported by the Russian Science Foundation (grant No 23-23-00446).

Conflict of interest

The authors declare that they have no conflict of interest.

References

- [1] L.E. Bausá, F. Jaque, J. Garcia Sole, A. Duran. *J. Mater. Sci.*, **23**, 1921 (1988). DOI: 10.1007/BF01115751
- [2] L.E. Bausá, I. Vergara, J. García-Solé, W. Streck, P.J. Deren. *J. Appl. Phys.*, **68**, 736 (1990). DOI: 10.1063/1.346807
- [3] P.F. Moulton. *OPN*, **8**, 9 (1982).
- [4] P.F. Moulton. *J. Opt. Soc. Am. B*, **3**, 125 (1986). DOI: 10.1364/JOSAB.3.000125
- [5] A. Sanchez, R.E. Fahey, A.J. Strauss, R.L. Aggarwal. *Opt. Lett.*, **11**, 363 (1986). DOI: 10.1364/ol.11.000363
- [6] P.W. Roth, A.J. Maclean, D. Burns, A.J. Kemp. *Opt. Lett.*, **36**, 304 (2011). DOI: 10.1364/OL.36.000304
- [7] P.F. Moulton, J.G. Cederberg, K.T. Stevens, G. Foundos, M. Koselja, J. Preclikova. *Opt. Mater. Express*, **9**(5), 2216 (2019). DOI: 10.1364/OME.9.002216
- [8] K. Morinaga, H. Yoshida, H. Takebe. *J. Am. Ceram. Soc.*, **77**, 3113 (1994). DOI: 10.1111/j.1151-2916.1994.tb04557.x
- [9] N.A. El-Shafi, M.M. Morsi. *J. Mater. Sci.*, **32**, 5185 (1997). DOI: 10.1023/A:1018685904770
- [10] L.H.C. Andrade, S.M. Lima, A. Novatski, A.M. Neto, A.C. Bento, M.L. Baesso, F.C.G. Gandra, Y. Guyot, G. Boulon. *Phys. Rev. B*, **78**, 224202 (2008). DOI: 10.1103/PhysRevB.78.224202
- [11] A. Jouini, H. Sato, A. Yoshikawa, T. Fukuda, G. Boulon, G. Panczer, K. Kato, E. Hanamura. *J. Mater. Res.*, **21**, 2337 (2006). DOI: 10.1557/jmr.2006.0280
- [12] A. Jouini, A. Yoshikawa, A. Brenier, T. Fukuda, G. Boulon. *Phys. Stat. Sol. C*, **4**(3), 1380 (2007). DOI: 10.1002/pssc.200673872
- [13] N.J. van der Laag, M.D. Snel, P.C.M.M. Magusin, G. de With. *J. Eur. Ceram.*, **24**(8), 2417 (2004). DOI: 10.1016/j.jeurceramsoc.2003.06.001
- [14] R.A. Fregola, H. Skogby, F. Bosi, V. D'Ippolito, G.B. Andreozzi, U. Hålenius. *Am. Mineral.*, **99**, 2187 (2014). DOI: 10.2138/am-2014-4962
- [15] G. Lorenzi, G. Baldi, F. Di Benedetto, V. Faso, P. Lattanzi, M. Romanelli. *J. Eur. Ceram. Soc.*, **26**(3), 317 (2006). DOI: 10.1016/j.jeurceramsoc.2004.10.027
- [16] J. Popović, E. Tkalčec, B. Gržeta, S. Kurajica, B. Rakvin. *Am. Mineral.*, **94**, 771 (2009). DOI: 10.2138/am.2009.3173
- [17] M.T. Tsai, Y.S. Chang, Y.H. Chou, K.M. Tsai. *J. Solid State Chem.*, **214**, 86 (2014). DOI: 10.1016/j.jssc.2013.10.019
- [18] P.J. Dereń, D. Stefańska, M. Ptak, M. Mączka, W. Walerczyk, G. Banach. *J. Am. Ceram. Soc.*, **97**(6), 1883 (2014). DOI: 10.1111/jace.12858
- [19] I. Alekseeva, A. Baranov, O. Dymshits, V. Ermakov, V. Golubkov, M. Tsenter, A. Zhilin. *J. Non-Cryst. Sol.*, **357**, 3928 (2011). DOI: 10.1016/j.jnoncrysol.2011.08.011
- [20] V.V. Golubkov, O.S. Dymshits, V.I. Petrov, A.V. Shashkin, M.Ya. Tsenter, A.A. Zhilin, U. Kang. *J. Non-Cryst. Sol.*, **351**, 711 (2005). DOI: 10.1016/j.jnoncrysol.2005.01.071
- [21] K. Ereemeev, O. Dymshits, I. Alekseeva, A. Khubetsov, S. Zapalova, M. Tsenter, L. Basyrova, P. Loiko, A. Zhilin, V. Popkov. *J. Phys. Conf. Ser.*, **1697**, 012125 (2020). DOI: 10.1088/1742-6596/1697/1/012125
- [22] K. Ereemeev, L. Basyrova, O. Dymshits, S. Balabanov, A. Belyaev, I. Alekseeva, A. Khubetsov, M. Tsenter, A. Volokitina, A. Zhilin, V. Popkov, P. Loiko. *J. Phys.: Conf. Ser.*, **2086**, 012138 (2021). DOI: 10.1088/1742-6596/2086/1/012138
- [23] P. Scherrer, *J. Abh. Akad. Wiss. Gött., Math.-Phys. Kl.*, **2**, 98 (1918).
- [24] V. Mohacek-Grosev, M. Vrankic, A. Maksimovic, V. Mandi. *J. Alloys Compd.*, **697**, 90 (2017). DOI: 10.1016/j.jallcom.2016.12.116
- [25] I.P. Alekseeva, O.S. Dymshits, V.V. Golubkov, P.A. Loiko, M.Ya. Tsenter, K.V. Yumashev, S.S. Zapalova, A.A. Zhilin. *J. Non-Cryst. Sol.*, **384**, 73 (2014). DOI: 10.1016/j.jnoncrysol.2013.05.038
- [26] A. Sanchez, A.J. Strauss, R.L. Aggarwal, R.E. Fahey. *IEEE J. Quantum Electron.*, **24**(6), 1002 (1988). DOI: 10.1109/3.220
- [27] A.S. Marfunin. *Physics of minerals and inorganic materials: an introduction* (Springer-Verlag, Berlin, Heidelberg, NY., 1979), 340 p.
- [28] B.M. Loeffler, R.G. Burns, J.A. Tossell, D.J. Vaughan, K.H. Johnson. *Proceedings of the Fifth Lunar Conf., Supplement 5, Geochim. Cosmochim. Acta*, **3**, 3007 (1974).
- [29] G.H. Faye, D.C. Harris. *Can. Mineral.*, **10**, 47 (1969).
- [30] R.G. Burns. *Ann. Rev. Earth Planet. Sci.*, **9**, 345 (1981). DOI: 10.1146/annurev.ea.09.050181.002021
- [31] H.St.C. O'Neill, W.A. Dollase. *Phys. Chem. Miner.*, **20**, 541 (1994). DOI: 10.1007/BF00211850
- [32] R. Reisfeld, A. Kisilev, E. Greenberg, A. Buch, M. Ish-Shalom. *Chem. Phys. Lett.*, **104**, 153 (1984). DOI: 10.1016/0009-2614(84)80186-4
- [33] P. Loiko, A. Belyaev, O. Dymshits, I. Evdokimov, V. Vitkin, K. Volkova, M. Tsenter, A. Volokitina, M. Baranov, E. Vilejshikova, A. Baranov, A. Zhilin. *J. Alloys Compd.*, **725**, 998 (2017). DOI: 10.1016/j.jallcom.2017.07.239
- [34] G. Boulon. *Mater. Chem. Phys.*, **16**, 301 (1987). DOI: 10.1016/0254-0584(87)90104-0

Translated by M.Verenikina